

<sup>1</sup>Chetan Bariya  
<sup>2</sup>Bhavik Brambhatt  
<sup>3</sup>Tejal Chaudhari  
<sup>4</sup>Sumit Banker  
<sup>5</sup>Mitesh Priyadarshi  
<sup>6</sup>Priyank Patel

## Indirect Field Oriented Control of Induction Motor



**Abstract:** - The control solutions employed for the inverter-fed induction motor have yielded satisfactory steady-state performance but inadequate dynamic response. Several effective control strategies have emerged to provide good performance in recent decades. In the context of high-performance AC electric machines and drives, field-oriented control emerges as a very consequential control methodology. Indirect field oriented control has emerged as a widely adopted industry standard for induction devices due to its simplicity and excellent reliability. The development of vector control techniques has made it possible to use an induction motor in high performance applications just like a separately stimulated dc motor. A PI controller may be used to regulate the speed since it can take the signaling speed and turn it into the control torque, which in turn determines the drive speed. This work presents an indirect field orientation control of a 3-phase 415V, 50Hz system based on a PI controller. A potential approach for utilizing a cascaded multilayer inverter in an induction motor is presented in Simulink/MATLAB.

**Keywords:** Cascaded inverter, Park's Transformation, Induction Motor, IFOC.

### I. INTRODUCTION

The three-phase induction motor serves as a crucial component in the modern industrial sector. Adjustable-speed drives frequently employ three-phase induction motors, which are characterized by the presence of stator and rotor windings in three-phase configurations. Induction machines may be classified into two main types: squirrel-cage and wound-rotor [1]. Squirrel-cage induction motors have a cylindrical rotor with rotor windings that are short-circuited, allowing the voltage to be delivered to the stator windings. Instead of a brush and commutator, the rotor is composed of conducting bars that are inserted into the rotor slots. The shorting rings are responsible for shorting these bars. Nevertheless, the utilization of wound-rotor induction motors has been limited due to their relatively lower efficiency and maximal angular velocity in comparison to squirrel-cage motors. In contrast, squirrel-cage induction motors have been extensively employed in high-performance electric drives and electromechanical systems throughout many applications. Hence, this article will only showcase a three-phase squirrel-cage induction motor drive in the simulator that has been designed and presented. At the specified speed and torque, the induction motor exhibits a notable level of efficiency. Nevertheless, while the motor is operating at low load, its efficiency significantly declines as a result of an imbalance between the losses incurred by the copper and core. Therefore, energy conservation may be attained by the appropriate choice of the flux level in the motor. The present study investigates the use of a PI controller for the indirect field-oriented control of an induction motor that is powered by a 3-level inverter and a 5-level cascaded inverter. The structure of this document is as follows: Section I provides an overview of the speed control techniques used for induction motors. In Section II, a mathematical model is presented for the indirect field-oriented control of an induction motor. In Section III, simulation results for a 3-level inverter and a 5-level cascaded inverter are shown. Once the research article has reached its conclusion,

<sup>1,3,4</sup> Electrical Engineering Department, Government Engineering College, Modasa, Arvalli, Modasa 383315, India

<sup>2,6</sup> E. C. Engineering Department, Government Engineering College, Modasa, Arvalli, Modasa 383315, India

<sup>5</sup> Electrical Engineering Department, L. D. College of Engineering, Ahmedabad 380015, India

<sup>1</sup>chetanbariya27@gmail.com, <sup>2</sup>bhavik0072009@gmail.com, <sup>3</sup>tejalchaudhari1986@gmail.com, <sup>4</sup>sumitvbanker@gmail.com, <sup>5</sup>mitesh\_343@yahoo.co.in, <sup>6</sup>pvp.fetr@gmail.com

Corresponding author: Chetan Bariya (chetanbariya27@gmail.com)

Copyright©JES2024on-line:journal.esrgroups.org

### A. Speed Control Methods of Induction Motor

- **Conventional Methods of Speed Control**

The possible methods of speed control may be

- (a) Varying the slip ( $s$ )
- (b) The number of pole-pairs ( $P$ ) or
- (c) The supply angular frequency ( $\omega$ )

- **Solid state speed control strategies**

With the invention of new power electronic devices induction motors are gaining majority in adjustable speed drives. The different speed control methods for induction motor drive are from stator side and rotor side

Stator side:

1. Variable voltage
2. Variable frequency
3. Constant V/f Control

Rotor side:

1. Rotor resistance control
2. Voltage injection method
3. Slip power recovery schemes

Popular method employed in adjustable speed drive is V/F control. This aims at maintaining constant flux over wide range of speed variation. In this control scheme the transient response of the machine is very poor, decoupling between flux and torque is not achieved in this. The advanced control methods are

1. Scalar control
2. Vector control

### B. Vector Control

This control is also known as the “field oriented control”, “flux oriented control” or “indirect torque control”. Using field orientation (Clarke-Park transformation), three-phase current vectors are converted to a two-dimensional rotating reference frame (d-q) from a three-dimensional stationary reference frame. The “d” component represents the flux producing component of the stator current and the “q” component represents the torque producing component. These two decoupled components can be independently controlled by passing through separate PI controllers. The outputs of the PI controllers are transformed back to the three-dimensional stationary reference plane using the inverse of the Clarke-Park transformation. The corresponding switching pattern is generating by hysteresis pulse width modulated.

This control simulates a separately excited DC motor model, which provides an excellent torque-speed curve. The transformation from the stationary reference frame to the rotating reference frame is done and controlled with reference to a specific flux linkage space vector (stator flux linkage, rotor flux linkage or magnetizing flux linkage). In general, there exists three possibilities for such selection and hence, three different vector controls. They are:

- Stator flux oriented control
- Rotor flux oriented control
- Magnetizing flux oriented control

As the torque producing component in this type of control is controlled only after transformation is done and is not the main input reference, such control is known as “indirect torque control”.

The most challenging and ultimately, the limiting feature of the field orientation, is the method whereby the flux angle is measured or estimated. Depending on the method of measurement, the vector control is divided into two subcategories: direct and indirect vector control. In direct vector control, the flux measurement is done by using the flux sensing coils or the Hall devices. This adds to additional hardware cost and in addition, measurement is not highly accurate. Therefore, this method is not a very good control technique. The more

common method is indirect vector control. In this method, the flux angle is not measured directly, but is estimated from the equivalent circuit model and from measurements of the rotor speed, the stator current and the voltage. One common technique for estimating the rotor flux is based on the slip relation. This requires the measurement of the rotor position and the stator current. With current and position sensors, this method performs reasonably well over the entire speed range. The most high-performance VFDs in operation today employ indirect field orientation based on the slip relation. The main disadvantage of this method is the need of the rotor position information using the shaft mounted encoder. This means additional wiring and component cost. This increases the size of the motor. When the drive and the motor are far apart, the additional wiring poses a challenge.

To overcome the sensor/encoder problem, today's main research focus is in the area of a sensor less approach. The advantages of the vector control are to better the torque response compared to the scalar control, full-load torque close to zero speed, accurate speed control and performance approaching DC drive, among others. But this requires a complex algorithm for speed calculation in real-time. Due to feedback devices, this control becomes costly compared to the scalar control.

## II. MATHEMATICAL MODEL OF INDIRECT VECTOR CONTROL OF INDUCTION MOTOR

Fig.1 shows a SIMULINK/MATLAB model of indirect vector control induction motor. A 3-phase, 1.1KW, 415V, 50 Hz induction motor is supplied through a current-controlled voltage source inverter (CC-VSI), realized through cascaded multilevel inverter. The gate drives for cascaded multilevel inverter are generated by PWM current regulator. The controller makes two stage of inverse transformation, as shown so that control current  $I_d^*, I_q^*$  correspond to machine current  $I_d, I_q$  respectively, in addition the unit vector assures correct alignment of  $I_d$  current with the flux vector  $\lambda_r$  and  $I_q$  perpendicular to it. The  $d_s - q_s$  axes are fixed on the stator, but the  $d_r - q_r$  axes are fixed on rotor, moving at speed  $\omega_r$ . Synchronously rotating axes  $d_e - q_e$  is rotating ahead of the  $d_r - q_r$  axes by the positive slip angle  $\theta_{sl}$  corresponding to slip frequency  $\omega_{sl}$ . Since the rotor pole is directed on the  $d_e$  axis and  $\omega_e = \omega_r + \omega_{sl}$ . The unit vector signal is determined as:

$$\theta_e = \int (\omega_r + \omega_{sl}) dt = \theta_r + \theta_{sl} \quad (1)$$

It is to be noted that the rotor pole position is not absolute, but is slipping with respect to the rotor at frequency  $\omega_{sl}$ .

For decoupling control, the stator flux component of current  $i_d$  should be aligned on the  $d_e$  axis, and the torque component of current  $I_q$  should be on the  $q_e$ . Control equation of indirect vector control can be written as (P.Vas and J.Li, 1993, B.K Bose, 2002):

$$R_r I_{qr} + \frac{d}{dt} \lambda_{qr} + (\omega_e - \omega_r) \lambda_{dr} = 0 \quad (2)$$

$$R_r I_{dr} + \frac{d}{dt} \lambda_{dr} + (\omega_e - \omega_r) \lambda_{qr} = 0 \quad (3)$$

The rotor flux linkage equation written as:

$$\lambda_{qr} = L_m I_{qs} + L_r I_{qr} \quad (4)$$

$$\lambda_{dr} = L_m I_{ds} + L_r I_{dr} \quad (5)$$

Therefore, the rotor d-q currents are:

$$I_{dr} = \frac{1}{L_r} \lambda_{dr} - \frac{L_m}{L_r} I_{ds} \quad (6)$$

$$I_{qr} = \frac{1}{L_r} \lambda_{qr} - \frac{L_m}{L_r} I_{qs} \quad (7)$$

The rotor currents can be further written in the form of rotor flux linkages:

$$\frac{d\lambda_{dr}}{dt} + \frac{R_r}{L_r} \lambda_{dr} - \frac{L_m}{L_r} R_r I_{ds} - \omega_{sl} \lambda_{qr} = 0 \quad (8)$$

$$\frac{d\lambda_{qr}}{dt} + \frac{R_r}{L_r} \lambda_{qr} - \frac{L_m}{L_r} R_r I_{qs} - \omega_{sl} \lambda_{dr} = 0 \quad (9)$$

Where,  $\omega_{sl} = \omega_e - \omega_r$

For decoupling control

$$\lambda_{qr} = 0 \quad (10)$$

$$\frac{d\lambda_{qr}}{dt} = 0 \quad (11)$$

Also the total rotor flux  $\widehat{\lambda}_r$  is directed on  $d_e$  axis:

$$\frac{L_r}{R_r} \frac{d\lambda_r}{dt} + \widehat{\lambda}_r = L_m I_{ds} \quad (12)$$

$$\omega_{sl} = \frac{L_m R_r}{\widehat{\lambda}_r L_m} I_{ds} \quad (13)$$

Where,  $\widehat{\lambda}_r = \lambda_{dr}$

If rotor flux =  $\widehat{\lambda}_r$  constant, which is usually the case equation.

$$\widehat{\lambda}_r = L_m I_{ds} \quad (14)$$

Therefore, the rotor flux is directly proportional to current  $i_{ds}$  in steady state.

#### A. Simulation of Indirect Field oriented control of induction motor

A block diagram of an indirect-vector-controlled (IVC) 3-phase 1.1 KVA, 50Hz induction motor drive is shown in Fig. 3. Incorporating the proposed PI speed controller. The feedback speed control loop generates the active or torque current command  $I_{qs}^*$ , as indicated. The vector rotator receives the torque and excitation current commands  $I_{qs}^*$  and  $I_{ds}^*$ , respectively. The induction motor is fed by a hysteresis current-controlled pulse width modulated (PWM) multilevel inverter. The motor currents are decomposed into  $I_d$  and  $I_q$  components which are respectively flux and torque components in the  $d-q$  reference frame rotating with the stator frequency  $\omega_s$ .

#### The various components of the proposed simulation project

- 5-level cascaded H-bridge inverter
- PI speed controller block
- Indirect vector control block
- Current regulator block

The motor speed  $\omega$  is compared to the reference  $\omega^*$  and the error is processed by the speed controller to produce a torque command  $T_e^*$ . The stator quadrature-axis current reference  $I_{qs}^*$  is calculated from torque reference  $T_e^*$  as

$$I_{qs}^* = \frac{2}{3} \cdot \frac{2}{p} \cdot \frac{L_r}{L_m} \cdot \frac{T_e^*}{|\lambda_r|_{est}} \quad (15)$$

Table 1: Parameters of three phase induction motor used in this study

Rotor Type	Squirrel cage
Reference frame	Synchronous
synchronous speed	1500 rpm
rated speed	1415 rpm
Nominal Power	1.1 KVA
Voltage Line to Line	415 V
Frequency	50 Hz
Stator resistance	6.03 ohm
Stator inductance	0.0299 H
Rotor resistance	6.085 ohm
Rotor inductance	0.0299 H
Mutual inductance	0.4893 H
Inertia	0.011787
Friction factor	0.000479
Number of poles	4

Where,  $L_r$  is the rotor inductance,  $L_m$  is the mutual inductance, and  $|\lambda_r|_{est}$  is the estimated rotor flux linkage given by

$$|\lambda_r|_{est} = \frac{L_m I_{ds}}{1 + \tau_r s} \quad (16)$$

Where,  $\tau_r = L_r/R_r$  is the rotor time constant.

The stator direct-axis current reference  $i_{ds}^*$  is obtained from rotor flux reference input  $|\lambda_r|^*$

$$i_{ds}^* = \frac{|\lambda_r|^*}{L_m} \quad (17)$$

The rotor flux position  $\theta_e$  required for coordinates transformation is generated from the rotor speed  $\omega_m$  and slip frequency  $\omega_{sl}$ :

$$\theta_e = \int (\omega_m + \omega_{sl}) dt \quad (18)$$

The slip frequency is calculated from the stator reference current  $i_{qs}^*$  and the motor parameters.

$$\omega_{sl} = \frac{L_m}{|\lambda_r|} \cdot \frac{R_r}{L_r} \cdot i_{qs}^* \quad (19)$$

The  $I_{qs}^*$  and  $I_{ds}^*$  current references are converted into phase current references  $I_a^*$ ,  $I_b^*$ ,  $I_c^*$  for the current regulators.

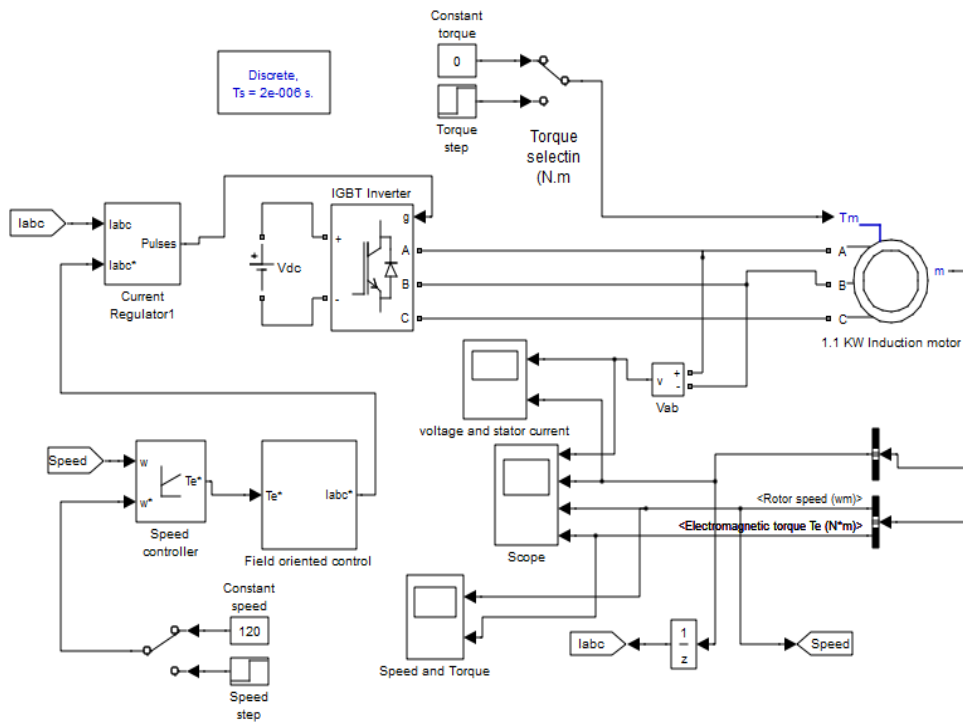


Fig. 3 Simulation model of indirect field oriented control for 3-phase Induction motor using 5-level inverter.

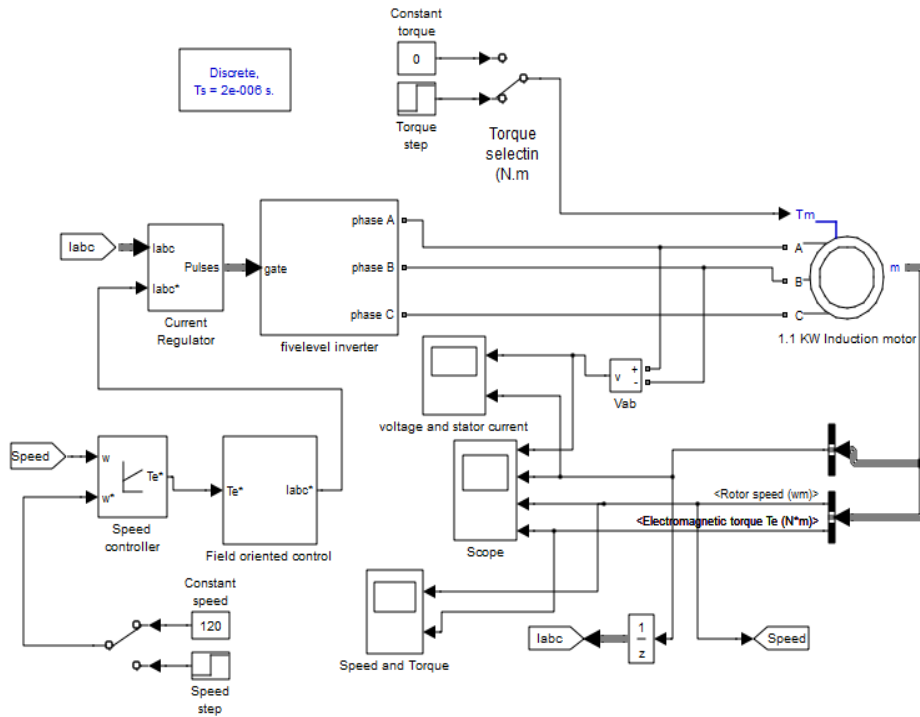


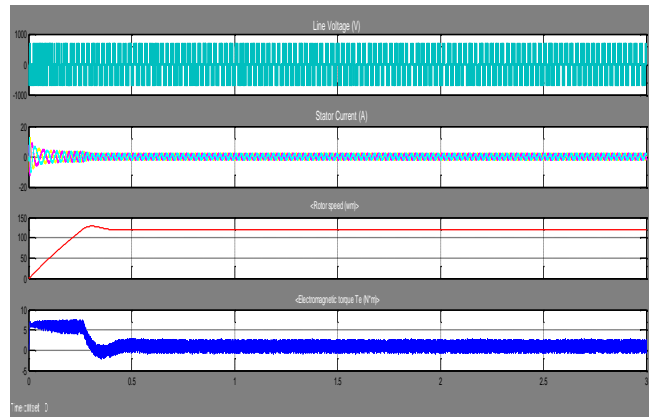
Fig. 3 Simulation model of indirect field oriented control for 3-phase Induction motor using 5-level inverter.

**2. Simulation Results**

*B.* Simulation result of indirect field oriented control of induction motor using 3-level inverter.

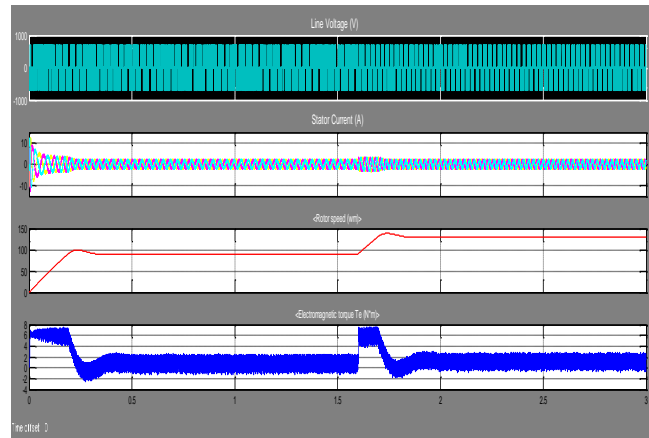
**Result 1.** When constant speed is apply

Constant Speed =120 rad/sec, Constant Torque =0 Nm, Simulation Time =3 sec



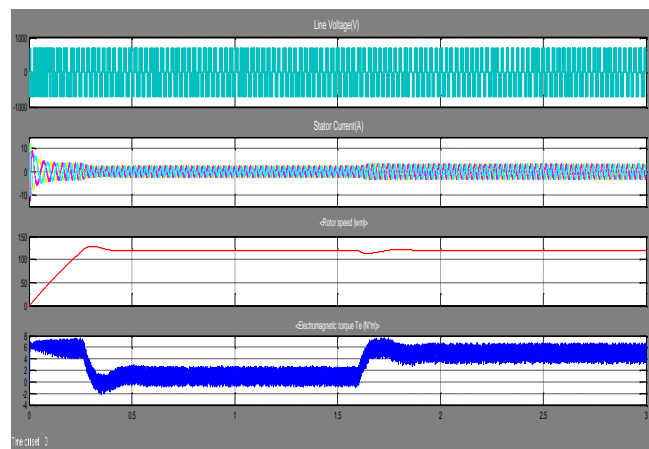
**Result 2.** When Step Speed is apply

Constant Torque =0 Nm, Simulation Time =3 sec, Initial Value =90 rad/sec, Final Value =130 rad/sec



**Result 3.** When Step Torque is apply

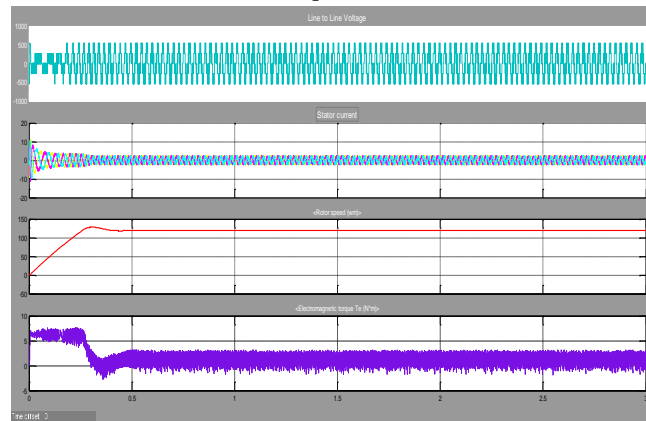
Constant Speed =120 rad/sec, Simulation Time=3sec, Initial Value =0 rad/sec, Final Value =4 rad/sec, Step time =1.6 s



C. Simulation result of indirect field oriented control of induction motor using 5-level cascaded inverter.

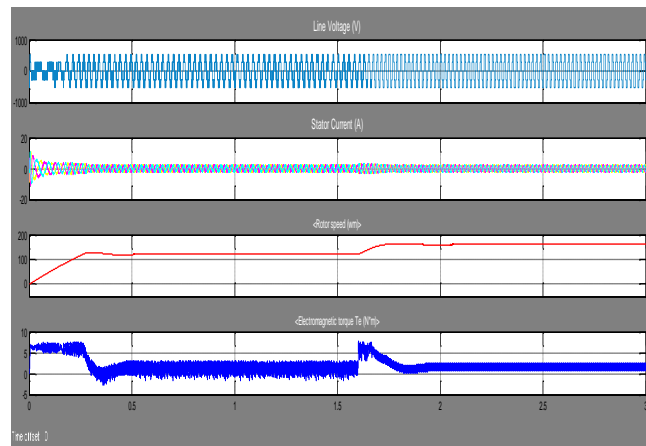
**Result 1.** When constant speed is apply

Constant Speed = 120 rad/sec, Constant Torque = 0 Nm, Simulation Time = 3 sec



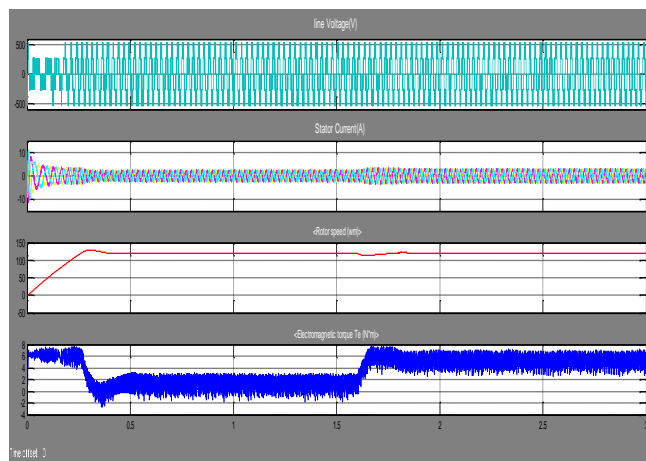
**Result 2.** When Step Speed is apply

Constant Torque = 0 Nm, Simulation Time = 3 sec, Initial Value = 90 rad/sec, Final Value = 130 rad/sec



**Result 3.** When Step Torque is apply

Constant Speed = 120 rad/sec, Simulation Time = 3 sec, Initial Value = 0 rad/sec, Final Value = 4 rad/sec, Step time = 1.6 s





### 3. Conclusion

In this paper cascaded 3-level and 5-level inverter fed 3-phase 415V, 50Hz Induction motor speed is controlled by Indirect Field Oriented control method (IFOC). Indirect Field Oriented control of induction motor fed by 5-level inverter had a faster speed response and less transient oscillations in terms of voltage, current, and torque compare to fed by 3-level inverter. Therefore, it gives better performance. The amplitudes of the transients are completely controlled by the IFOC method. With the use of IFOC method using 5-level cascaded inverter we get the smoother speed control of the induction motor. So, Induction motor operates like a separately excited dc motor.

### REFERENCES

1. B.K. Bose, P Electronics and AC Drives, Prentice-Hall, Englewood Cliffs, New Jersey, 1986
2. Baburaj, Karanayil, Rahman Muhammed Fazlur, and Grantham Colin. "Identification of Induction Motor Parameters in Industrial Drives with Artificial Neural Networks." *Advances in Fuzzy Systems* (2009).
3. Soe, Nyein Nyein, Thet Thet Han Yee, and Soe Sandar Aung. "Dynamic modeling and simulation of three-phase small power induction motor." *World Academy of Science, Engineering and Technology* 42.79 (2008): 421-424.
4. Ayasun, Saffet, and Chika O. Nwankpa. "Induction motor tests using MATLAB/Simulink and their integration into undergraduate electric machinery courses." *IEEE Transactions on education* 48.1 (2005): 37-46.
5. Ohm, Dal Y. "Dynamic model of induction motors for vector control." *Drivetech, Inc., Blacksburg, Virginia* (2001): 1-10.
6. Ansari, A. A., and D. M. Deshpande. "Mathematical model of asynchronous machine in MATLAB Simulink." *International Journal of Engineering Science and Technology* 2.5 (2010): 1260-1267. "Electrical motor drives" – modeling, analysis, and control by R. Krishnan, Prentice-Hall, Englewood Cliffs, New Jersey, 1986
7. Corzine, K. A., S. D. Sudhoff, and C. A. Whitcomb. "Performance characteristics of a cascaded two-level converter." *IEEE Transactions on Energy Conversion* 14.3 (1999): 433-439.
8. Muhammad, H. Rashid. "Power Electronics-Circuits, Devices, and Applications." *Upper Saddle River, NJ, Pearson Prentice Hall* (2004).
9. Rodriguez, Jose, Jih-Sheng Lai, and Fang Zheng Peng. "Multilevel inverters: a survey of topologies, controls, and applications." *IEEE Transactions on industrial electronics* 49.4 (2002): 724-738.
10. Kashappa, Neelashetty, and K. Ramesh Reddy. "Comparison of 3-level and 9-level inverter-fed induction motor drives." *Research Journal of Applied Sciences, Engineering and Technology* 3.2 (2011): 123-131.
11. Shi, K. L., et al. "Modelling and simulation of the three-phase induction motor using Simulink." *International journal of electrical engineering education* 36.2 (1999): 163-172.
12. Singh, Girish Kumar, et al. "A simple indirect field-oriented control scheme for multiconverter-fed induction motor." *IEEE Transactions on industrial electronics* 52.6 (2005): 1653-1659.
13. Zhang, Yu, Zhenhua Jiang, and Xunwei Yu. "Indirect field-oriented control of induction machines based on synergetic control theory." *2008 IEEE Power and Energy Society General Meeting-Conversion and Delivery of Electrical Energy in the 21st Century*. IEEE, 2008.
14. Shrawane, Prasad. "Indirect field-oriented control of induction motor." *12th IEEE International Power Electronics Congress*. IEEE, 2010.
15. Brahmabhatt, Bhavik, and Hina Chandwani. "Tuning and experimental assessment of second-order generalized integrator–frequency locked loop grid synchronization for single-phase grid assisted system." *IOP Conference Series: Materials Science and Engineering*. Vol. 1045. No. 1. IOP Publishing, 2021.  
Brahmabhatt, Bhavik, and Hina Chandwani. "Single phase transformerless photovoltaic inverter with reactive power control." *2016 IEEE 1st International Conference on Power Electronics, Intelligent Control and Energy Systems (ICPEICES)*, IEEE, 2016.
16. Brahmabhatt, Bhavik, and Hina Chandwani. "Grid Synchronization for Three-Phase Grid-Tied Converter Using Decouple-Second-Order Generalized Integrator." *Proceedings of the International e-Conference on Intelligent Systems and Signal Processing: e-ISSP 2020*. Springer Singapore, 2022.
17. Brahmabhatt, B., and H. Chandwani. "Modified second order generalized integrator-frequency locked loop grid synchronization for single phase grid tied system tuning and experimentation assessment." *International Journal of Engineering*, Vol.35(2)(2022): 283-290.
18. Brahmabhatt, B. A., and H. Chandwani. "Experimental assessment of Single Phase Grid assisted system using Second Order Generalized Integrator–Frequency Locked Loop." *Indian Journal of Science and Technology* 14.5 (2021): 445-456.